

# A photostable fluorescent probe for targeted imaging of tumour cells possessing integrin $\alpha_v\beta_3$ \*\*†

Liqin Xiong,<sup>a</sup> Mengxiao Yu,<sup>a</sup> Mingjun Cheng,<sup>b</sup> Meng Zhang,<sup>a</sup> Xiaoyan Zhang,<sup>b</sup> Congjian Xu<sup>\*b</sup> and Fuyou Li<sup>\*a</sup>

Received 17th November 2008, Accepted 16th December 2008

First published as an Advance Article on the web 7th January 2009

DOI: 10.1039/b820576k

**A one-step  $S_NAr^H$  reaction has been used for the synthesis of photostable probe **2**, which has good water solubility and low cytotoxicity; this probe can be used for targeted imaging of tumour cells by virtue of specific binding between integrin  $\alpha_v\beta_3$  and an arginine–glycine–aspartic acid tripeptide sequence.**

Fluorescence imaging is emerging as a powerful tool in bioscience and medicine because it provides a facile method for studying diseases at the cellular and molecular level.<sup>1</sup> Recently, the targeted imaging of specific molecular structures using fluorescent probes has attracted much interest, such as targeted imaging of the cell adhesion molecule integrin  $\alpha_v\beta_3$ .<sup>2–5</sup> Integrin  $\alpha_v\beta_3$  is a viable target for non-invasive imaging of invasive tumours, it is significantly up-regulated in activated endothelial cells and fast-growing solid tumour cells compared to its minimum expression in quiescent blood vessels and most normal tissues. Integrin  $\alpha_v\beta_3$  binds extracellular matrix molecules such as vitronectin, which contain the amino acid sequence Arg–Gly–Asp (RGD).<sup>3</sup> For these reasons, many molecular fluorescent probes containing the RGD motif, including organic probes such as the Cy dyes,<sup>4</sup> and semiconductor quantum dots (QDs),<sup>5</sup> have been developed for targeted imaging of integrin  $\alpha_v\beta_3$  expression. However, for application in biological fields, an ideal probe should display water-solubility, low cytotoxicity, cell-permeability and photostability.<sup>6</sup> Unfortunately, conventional organic dyes are still prone to photobleaching, which limits their extensive use and efficient application,<sup>7</sup> while QDs are controversial due to their inherent toxicity and chemical instability.<sup>8</sup> Therefore, it is necessary to develop fluorescent probes with low cytotoxicity and high photostability.

As a novel electron-deficient heterocycle, 8-oxo-8*H*-acnaphtho[1,2-*b*]pyrrole-9-carbonitrile **1** (Scheme 1) can react with N, O, or S nucleophiles by nucleophilic aromatic substitution ( $S_NAr^H$ ).<sup>9</sup> By virtue of its reaction with the –SH of cysteine/homocysteine, **1** has recently been used as a fluorescent sensor for Cys/Hcy, showing a 75-fold fluorescence enhancement.<sup>9b</sup> In the work described herein, the non-fluorescent compound **1** has been easily converted into the intensely

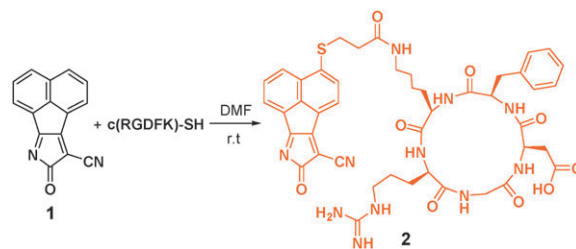
fluorescent probe **2** by means of an  $S_NAr^H$  reaction with the thiolated RGD peptide cyclo(Arg–Gly–Asp–Phe–Lys(mpa)) (c(RGDFK)-SH). Importantly, probe **2** exhibits good water solubility and low cytotoxicity, and furthermore can be used in the targeted imaging of integrin  $\alpha_v\beta_3$  expression in tumour cells.

Probe **2** was easily synthesized by stirring **1** and c(RGDFK)-SH in DMF for 2 h at room temperature, and was purified by reversed-phase preparative HPLC. The purity of **2** was 95.5% according to analytical reversed-phase HPLC analysis (Fig. S1†). The HPLC retention time of **2** was found to be 6.028 min ( $C_{45}H_{49}N_{11}O_9S$ , calculated 920.34; found 920.3 [ $M + H$ ]<sup>+</sup>).

As shown in Fig. 1, probe **2** exhibits a broad UV-vis band with a maximum at a wavelength of 512 nm, which may be assigned to intramolecular charge-transfer between the SH (donor) and carbonitrile (acceptor). It should be noted that an obvious red-shift of 74 nm was observed for the maximum absorption wavelength of **2** in comparison with that of **1**, corresponding to an apparent colour change from yellow-green to red (Fig. 1). Probe **2** emitted a distinctive orange-red fluorescence ( $\lambda_{max}^{em} = 570$  nm) under excitation with visible light at 515 nm. Importantly, compared with non-fluorescent compound **1** ( $\phi < 0.1\%$ ), the quantum efficiency of **2** in DMSO–phosphate buffer solution (PBS) (pH 7.3; 1 : 119, v/v) was 0.11 with reference to rhodamine B as a standard.<sup>10</sup>

To investigate the cytotoxicity of **2**, an MTT [3-(4,5-dimethylthiazol-2-yl)-2,5-diphenyltetrazolium bromide] assay with the human hepatocellular carcinoma cell line SMMC-7721 was used to determine the effect of **2** on cell proliferation after 24 h. No significant differences in the proliferation of the cells were observed in the absence or presence of 5–100  $\mu M$  **2** (Fig. 2). The cellular viabilities were estimated to be greater than 85% after 24 h. These data show that **2** ( $\leq 100 \mu M$ ) can be considered to have low cytotoxicity. The good water solubility and low cytotoxicity implied that **2** could serve as a potential fluorescence probe for targeted imaging.

To demonstrate that **2** can indeed act as a specific ligand for the  $\alpha_v\beta_3$  integrin receptor, the binding and subcellular



Scheme 1 Synthesis of **2**.

<sup>a</sup> Department of Chemistry & Laboratory of Advanced Materials, Fudan University, Shanghai, 200433, P. R. China.

E-mail: fyli@fudan.edu.cn; Fax: +86-21-55664621;

Tel: +86-21-55664185

<sup>b</sup> The Obstetrics and Gynecology Hospital, Fudan University, Shanghai, 200433, P. R. China. E-mail: xucj@hotmail.com

† Electronic supplementary information (ESI) available: Experimental procedures and characterization of **2**. Movie showing the photostability of **2**. See DOI: 10.1039/b820576k

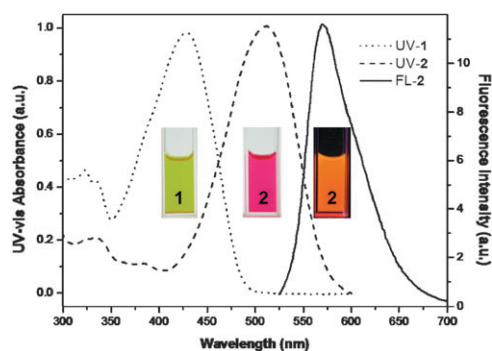


**Fig. 1** UV-vis absorption spectra of **1** and **2** in DMSO (10  $\mu\text{M}$ ) and the room temperature fluorescence spectrum ( $\lambda_{\text{ex}} = 515 \text{ nm}$ ) of 5  $\mu\text{M}$  **2** in DMSO–PBS (1 : 119, v/v). Photographs (inset) show the corresponding colour difference between **1** and **2**, the fluorescence photograph of **2** was obtained under 365 nm UV excitation.

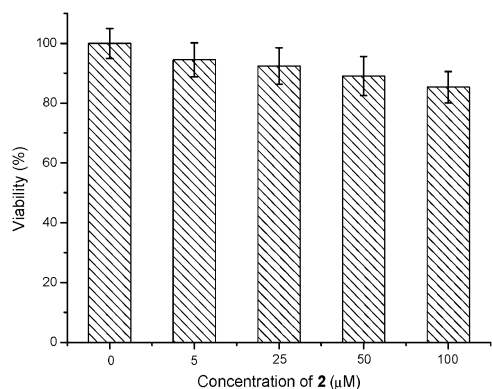


**Fig. 2** Cell viability values (%) estimated by MTT proliferation test *versus* incubation concentrations of **2**. Cells were incubated with 5–100  $\mu\text{M}$  **2** at 37  $^{\circ}\text{C}$  for 24 h.

localization of **2** were examined using an OLYMPUS FV1000 laser scanning microscope. We chose two cell lines, human cervical carcinoma HeLa cells,<sup>11</sup> which are known to possess integrin  $\alpha_v\beta_3$ , and human hepatocellular carcinoma SMMC-7721 cells as a control. As shown in Fig. 3, a strong fluorescence signal was observed in the HeLa cells (Fig. 3a), whereas the SMMC-7721 cells showed much less fluorescence (Fig. 3b). Moreover, the fluorescence intensity of **2** obtained from the live HeLa cells was higher than that obtained from the SMMC-7721 cells (Fig. S2<sup>†</sup>). These results imply that the HeLa cells express a higher amount of integrin  $\alpha_v\beta_3$  than the SMMC-7721 cells. It is known that integrin  $\alpha_v\beta_3$  receptors can be rapidly transported through the early endosomes, arriving at the perinuclear compartments approximately 30 min after endocytosis.<sup>12</sup> This phenomenon is consistent with our observation of the accumulation of **2** in the perinuclear region after 30 min of incubation at 37  $^{\circ}\text{C}$  (Fig. 3a). Such an endocytosis mechanism can be blocked at 4  $^{\circ}\text{C}$ . In a separate experiment, the HeLa cells were therefore loaded with **2** at 4  $^{\circ}\text{C}$  for 30 min and, as expected, only weak fluorescence was observed (Fig. 3c). This result supports the view that **2** is likely to enter the cells by this endocytotic uptake mechanism. The integrin receptor specificity of **2** could be further confirmed by a competition assay. The HeLa cells were pre-incubated with a tenfold excess of unlabelled c(RGDFK) peptide at 37  $^{\circ}\text{C}$  for

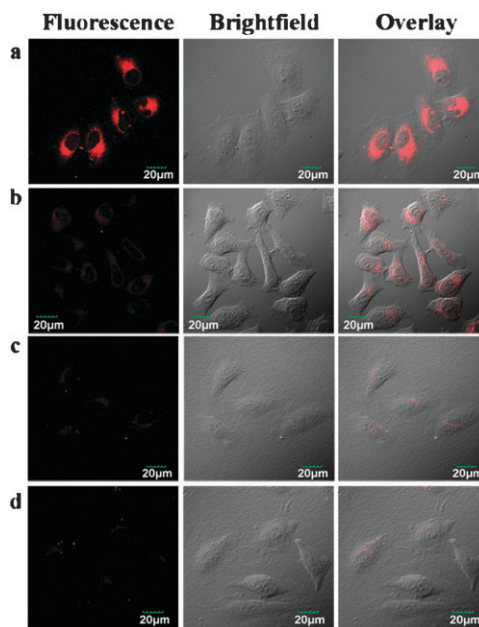


**Fig. 3** Confocal fluorescence images of 20  $\mu\text{M}$  **2** incubated with HeLa cells (a) or SMMC-7721 cells (b) for 30 min at 37  $^{\circ}\text{C}$  in DMSO/PBS (1 : 119, v/v). Incubation with HeLa cells at 4  $^{\circ}\text{C}$  (c) or in the presence of unlabeled c(RGDFK) peptide (d) were also shown.

30 min and then incubated with **2** at 37  $^{\circ}\text{C}$  for 30 min. As a result, almost no fluorescence signal was observed (Fig. 3d).

Additionally, the cellular uptake characteristics of **2** were investigated by means of flow cytometry. Upon excitation at 488 nm, HeLa cells incubated with **2** at 37  $^{\circ}\text{C}$  for 30 min displayed high emission intensities, while the emission intensities of SMMC-7721 cells treated with **2** were lower (Fig. 4a). Increasing the incubation time to 2 h, the HeLa cells still showed a higher uptake of **2** than the SMMC-7721 cells (Fig. 4b), confirming that the HeLa cells express a higher amount of integrin  $\alpha_v\beta_3$  than the SMMC-7721 cells. Thus, the results of confocal microscopy and flow cytometry studies demonstrated that **2** can target tumour cells possessing integrin  $\alpha_v\beta_3$ .

As is well known, the photobleaching characteristics of fluorescent materials are critical to their application as bio-probes. In the present study, the photostability of **2** was investigated by comparison with that of acridine orange<sup>6</sup> (an organic dye) under the same excitation conditions. To distinguish their staining regions, **2** and acridine orange were chosen to stain the cytoplasm and nuclei, respectively, of live SMMC-7721 cells. After continuous excitation at 488 nm with a high focal power (1.1 mW) for 200 s, the fluorescence intensity of acridine orange (520  $\pm$  20 nm, region-1, channel-1) decreased to 6% of its initial value, as shown in Fig. 5 (Fig. S3 and movie<sup>†</sup>). In contrast, the fluorescence intensity of **2** (580  $\pm$  20 nm, region-2, channel-2) still remained at 60% of the original value during the same period of excitation. These data established that **2** was more photostable than acridine orange. Furthermore, the chemical stability of **2** was confirmed by the fact that the stable fluorescence intensity in DMSO–PBS (1 : 119, v/v) was kept for a few days (Fig. S4<sup>†</sup>).

In conclusion, we have developed a photostable fluorescent probe **2** that was synthesized by the one-step  $\text{S}_{\text{N}}\text{Ar}^{\text{H}}$  reaction

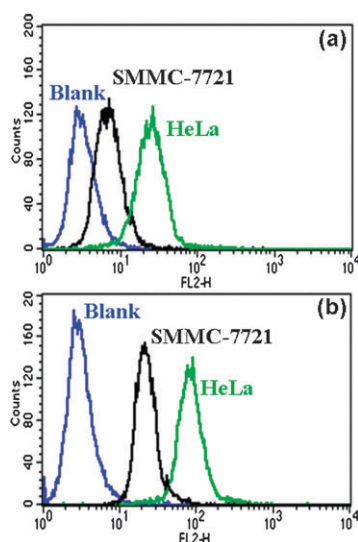


**Fig. 4** Flow cytometric histogram profiles of cellular uptake of **2** in HeLa cells and SMMC-7721 cells. The *x* axis indicates the log of the fluorescence intensity and the *y* axis indicates the number of cells. Cells were incubated with 20  $\mu\text{M}$  **2** in DMSO–PBS (1 : 119, v/v) at 37  $^{\circ}\text{C}$  for 30 min (a) and 2 h (b). Blue line indicates the emission intensities of SMMC-7721 cells in the absence of **2**.

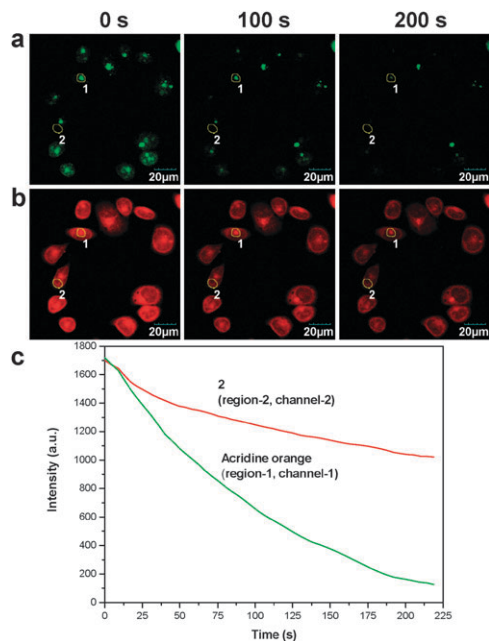


**Fig. 5** Comparison of **2** and acridine orange for resistance to photobleaching. Confocal fluorescence images of SMMC-7721 cells stained with **2** (a) and acridine orange (b) under continuous excitation at 488 nm with different laser scan times (0, 100, 200 s). (c) Fluorescence decay curves of **2** and acridine orange during the same period. The signals of acridine orange and **2** were collected from the region-1 of channel-1 (520  $\pm$  20 nm) and region-2 of channel-2 (580  $\pm$  20 nm), respectively. Cells were incubated at 37  $^{\circ}\text{C}$  for 1 h.

of **1** and thiolated RGD peptide c(RGDFK)-SH. Probe **2** has good water solubility and low cytotoxicity. Moreover, through specific binding of integrin  $\alpha_v\beta_3$  to the RGD tripeptide sequence, **2** can be used for targeted imaging of tumour cells possessing integrin  $\alpha_v\beta_3$ . The findings open up new perspectives

for integrin-targeted fluorescence imaging and suggest that **2** has great potential in imaging-guided cancer diagnosis.

The authors thank NSFC (20825101, 20775017 and 20501006), NCET-06-0353, and Shanghai Leading Academic Discipline Project (B108) for financial support.

## References

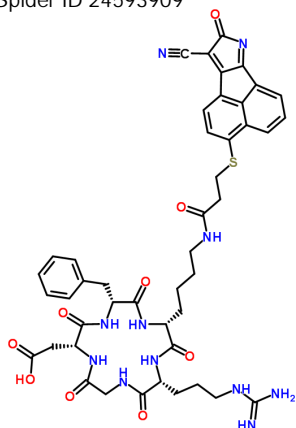
- (a) D. J. Stephens and V. J. Allan, *Science*, 2003, **300**, 82–86; (b) J. W. Lichtman and J. A. Conchello, *Nat. Methods*, 2005, **2**, 910–919; (c) B. D. Lourdes, N. R. David and C. C. Mercedes, *Chem. Soc. Rev.*, 2007, **6**, 993–1017; (d) W. M. Leevy, S. T. Gammon, H. Jiang, J. R. Johnson, D. J. Maxwell, E. N. Jackson, M. Marquez, D. Piwnica-Worms and B. D. Smith, *J. Am. Chem. Soc.*, 2006, **128**, 16476–16477; (e) D. Srikun, E. W. Miller, D. W. Domaille and C. J. Chang, *J. Am. Chem. Soc.*, 2008, **130**, 4596–4597.
- (a) J. W. Smith and D. A. Cheres, *J. Biol. Chem.*, 1990, **265**, 2168–72; (b) E. Ruoslahti, *Annu. Rev. Cell Dev. Bi.*, 1996, **12**, 697–715; (c) A. Meyer, J. Auernheimer, A. Modlinger and H. Kessler, *Curr. Pharm. Des.*, 2006, **12**, 2723–2747.
- (a) J. M. M. Willem, J. S. Gustav, W. H. Jo, J. W. B. Egbert, W. J. Daisy, S. Gert, A. K. Gerben, W. G. Arjan and N. Klaas, *FASEB J.*, 2005, **19**, 2008–2010; (b) Z. Hu, F. Luo, Y. Pan, C. Hou, L. Ren, J. Chen, J. Wang and Y. Zhang, *J. Biomed. Mater. Res., Part A*, 2007, 797–807; (c) M. Xavier, F. Martin, M. Karin, W. Ralph and J. Lee, *J. Med. Chem.*, 2006, **49**, 6087–6093; (d) A. M. Eric, K. M. Bharat, A. B. Leo, M. Milan, M. W. Sara, L. F. Kimberly, W. Wolfgang and A. C. David, *Proc. Natl. Acad. Sci. U. S. A.*, 2008, **27**, 9343–9348; (e) S. Petersen, J. M. Alonso, A. Specht, P. Duodu, M. Goeldner and A. Campo, *Angew. Chem., Int. Ed.*, 2008, **47**, 3192–3195.
- (a) S. Achilefu, S. Bloch, M. A. Markiewicz, T. X. Zhong, Y. P. Ye, R. B. Dorshow, B. Chance and K. X. Liang, *Proc. Natl. Acad. Sci. U. S. A.*, 2005, **102**, 7976–7981; (b) X. Y. Chen, P. S. Conti and R. A. Moats, *Cancer Res.*, 2004, **64**, 8009–8014; (c) A. V. Wallbrunn, C. Hölte, M. Zühlendorf, W. Heindel, M. Schäfers and C. Bremer, *Eur. J. Nucl. Med. Mol. Imag.*, 2007, **34**, 745–754; (d) Y. P. Ye, S. Bloch, B. G. Xu and S. Achilefu, *J. Med. Chem.*, 2006, **49**, 2268–2275; (e) Z. H. Jin, J. Razkin, V. Josserand, D. Boturyn, A. Grichine, I. Texier, M. C. Favrot, P. Dumy and J. L. Coll, *Mol. Imaging*, 2007, **6**, 43–55; (f) Z. Cheng, Y. Wu, Z. M. Xiong, S. S. Gambhir and X. Y. Chen, *Bioconjugate Chem.*, 2005, **16**, 1433–1441.
- (a) W. B. Cai, D. W. Shin, K. Chen, O. Gheysens, Q. Z. Cao, S. X. Wang, S. S. Gambhir and X. Y. Chen, *Nano Lett.*, 2006, **6**, 669–676; (b) B. R. Smith, Z. Cheng, A. De, A. L. Koh, R. Sinclair and S. S. Gambhir, *Nano Lett.*, 2008, **8**, 2599–2606.
- www.probes.com and www.invitrogen.com: R. P. Haugland, in *A Guide to Fluorescent Probes and Labelling Technologies*, Molecular Probes, Eugene, Oregon, 10th edn, 2005.
- (a) M. Bruchez Jr., M. Moronne, P. Gin, S. Weiss and A. P. Alivisatos, *Science*, 1998, **281**, 2013–2016; (b) M. X. Yu, Q. Zhao, L. X. Shi, F. Y. Li, Z. G. Zhou, H. Yang, T. Yi and C. H. Huang, *Chem. Commun.*, 2008, 2115–2117.
- (a) B. Dubertret, P. Skourides, D. J. Norris, V. Noireaux, A. H. Brivanlou and A. Libchaber, *Science*, 2002, **298**, 1759–1762; (b) I. L. Medintz, H. T. Uyeda, E. R. Goldman and H. Mattoussi, *Nat. Mater.*, 2005, **4**, 435–446; (c) X. Michalet, F. F. Pinaud, L. A. Bentolila, J. M. Tsay, S. Doose, J. J. Li, G. Sundaresan, A. M. Wu, S. S. Gambhir and S. Weiss, *Science*, 2005, **307**, 538–544.
- (a) Y. Xiao, F. Liu, X. Qian and J. Cui, *Chem. Commun.*, 2005, 239–241; (b) F. Liu, Y. Xiao, X. Qian, Z. Zhang, J. Cui, D. Cui and R. Zhang, *Tetrahedron*, 2005, **61**, 11264–11269; (c) M. Zhang, M. X. Yu, F. Y. Li, M. W. Zhu, M. Y. Li, Y. H. Gao, L. Li, Z. Q. Liu, J. P. Zhang, D. Q. Zhang, T. Yi and C. H. Huang, *J. Am. Chem. Soc.*, 2007, **129**, 10322–10323; (d) A. Coskun, M. D. Yilmaz and E. U. Akkaya, *Tetrahedron Lett.*, 2006, **47**, 3689–3691.
- N. Filipescu, G. W. Mushrush, C. R. Hurt and N. McAvoy, *Nature*, 1966, **211**, 960.
- M. Oba, S. Fukushima, N. Kanayama, K. Aoyagi, N. Nishiyama, H. Koyama and K. Kataoka, *Bioconjugate Chem.*, 2007, **18**, 1415–1423.
- M. Roberts, S. Barry, A. Woods, P. V. D. Sluijs and J. Norman, *Curr. Biol.*, 2001, **11**, 1392–1402.

## Primary compounds

SNRQMMAXXKPLKK-SEVDZJIVSA-N

compound no. 2

ChemSpider ID 24593909

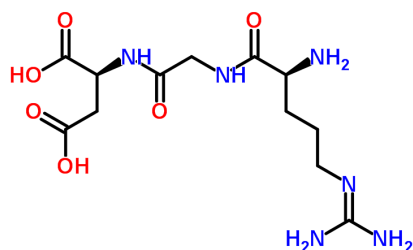


## Secondary compounds

IYMAXBFPHPZYIK-BQBZGAKWSA-N

RGD

ChemSpider ID 94603

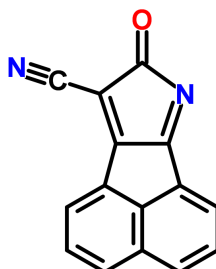


VQYSTSIAUDPRJH-UHFFFAOYSA-N

8-oxo-8H-acenaphtho[1,2-b]pyrrole-9-carbonitrile

compound no. 1

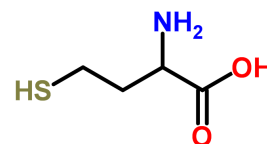
ChemSpider ID 24593910



FFFHZYDWPBMWHY-UHFFFAOYSA-N

homocysteine

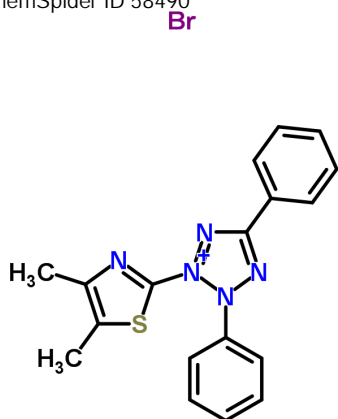
ChemSpider ID 757



AZKSAVLVSZKNRD-UHFFFAOYSA-M

MTT

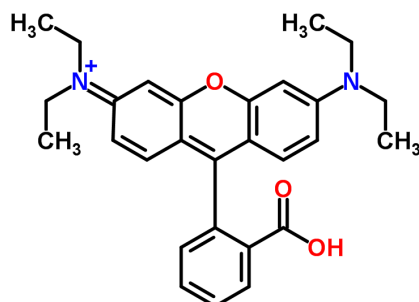
ChemSpider ID 58490



CVAVMIODJQHEEH-UHFFFAOYSA-O

rhodamine B

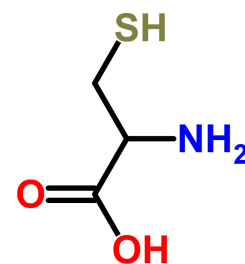
ChemSpider ID 6440



XUJNEKJLAYXESH-UHFFFAOYSA-N

cysteine

ChemSpider ID 574



## Routine compounds

XLYOFNOQVPJJNP-UHFFFAOYSA-N

water

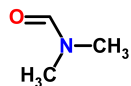
ChemSpider ID 937



ZMXDDKWLCZADIW-UHFFFAOYSA-N

DMF

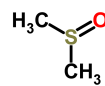
ChemSpider ID 5993



IAZDPXIOMUYVGZ-UHFFFAOYSA-N

DMSO

ChemSpider ID 659



DPKHZNPWBDQZCN-UHFFFAOYSA-N

acridine orange

ChemSpider ID 56136

